Proc. NIPR Symp. Antarct. Meteorites, 7, 73–93, 1994

A MINERALOGICAL STUDY OF THE PROPOSED PAIRED EUCRITES Y-792769 AND Y-793164 WITH REFERENCE TO CRATERING EVENTS ON THEIR PARENT BODY

Hiroshi TAKEDA[1], Akira YAMAGUCHI[1], L. E. NYQUIST[2] and D. D. BOGARD[2]

[1] *Mineralogical Institute, Faculty of Science, University of Tokyo, Hongo, Bunkyo-ku, Tokyo 113*
[2] *Mail Code SN, NASA Johnson Space Center, Houston, Texas 77058, U.S.A.*

Abstract: A comparison of the mineralogy of Yamato (Y-)792769 and Y-793164 has been performed to confirm the proposed pairing of these two specimens and to correlate their common shock-sintered textures with the resetting of their isotopic ages. The matrices of the two meteorites share this common texture as described for Y-792769, but their clast types are different. Y-792769 contains pyroxene fragments with Mg-rich compositions, which are not present in the matrix. A large basaltic clast present in Y-793164 includes acicular plagioclase crystals replacing the pyroxene grains. Pyroxene clasts in the matrix of the two meteorites showed a small compositional range between 30 and 45 in $Mg \times 100/(Mg+Fe)$ mol% and are similar to the more comminuted matrix pyroxenes, but lithic clast pyroxenes are uniform in bulk chemistry within a single clast type. The event which produced these monomict eucrites with minor compositional differences may have taken place earlier than the reset ^{39}Ar-^{40}Ar age of 3.99 Ga previously found for Y-792769. Some pyroxenes are more Fe-rich than those of common monomict eucrites such as Juvinas. The common pyroxene components and the shock-sintered textures support the proposed pairing of Y-792769 and Y-793164. Rb and Sr abundances and isotopic data do not strongly support the proposed pairing of the meteorites, but could be consistent with observed compositional heterogeneities within and between them. Sm and Nd abundances and isotopic data are similar for matrix samples of the meteorites and are consistent with their pairing.

1. Introduction

Yamato (Y-)792769, a polymict eucrite, is one of the largest eucrites in the Yamato collection and shows a compact fine-grained texture on the cut surface (YANAI and KOJIMA, 1987). This texture is quite different from that of the typical polymict eucrite (Y-74159 type) in the Yamato collection. The chemical compositions of pyroxenes within a single clast type in Y-792769 are nearly uniform (TAKEDA, 1991), unlike the case for Y-74159 type polymict eucrites (DELANEY *et al.*, 1984). A thin section photograph of Y-793164,65–1 in the Photographic Catalog of Antarctic Meteorites (Photo 292, YANAI and KOJIMA, 1987) suggests that it has a very different texture from that of Y-792769 (BOGARD *et al.*, 1993). However, the

cosmic ray exposure ages and terrestrial ages of Y-792769 and Y-793164 reported by MIURA *et al.* (1993) suggest their pairing. We investigated Y-793164,65–1 and a new polished thin section of this meteorite to define the variation in textural features and to confirm the proposed pairing of Y-792769 and Y-793164. We also discuss the cratering history of their parent body in conjunction with their sintered matrix texture and the presence of glassy veins and the ^{39}Ar-^{40}Ar age of Y-792769, which was reset at 3.99 Ga (BOGARD *et al.*, 1993). ^{39}Ar-^{40}Ar studies of Y-793164 are in progress.

The geochemistry and petrology of a small thin section of Y-793164 indicated that it is a monomict eucrite intermediate in composition between main-group eucrites and Nuevo Laredo (MITTLEFEHLDT and LINDSTROM, 1993). If Y-792769 and Y-793164 are indeed paired, Y-793164 should be polymict. Because local heterogeneity may be responsible for these apparently different textures, we investigated polished thin sections of Y-792769 made from chips located far from those studied previously. The very large size of Y-792769 makes it well suited for this kind of investigation.

Mineralogical characteristics of Y-792769 are summarized as follows: (1) Y-792769 is a polymict breccia containing pyroxenes with a limited range in chemical compositions; (2) compared to other Yamato polymict eucrites, Y-792769 includes fewer and smaller eucritic clasts with homogenized pyroxenes (BOGARD *et al.*, 1993); and (3) its fine-grained matrix is shock-compacted and sintered. This characteristic texture has been interpreted as having originated at the time defined by the totally reset ^{39}Ar-^{40}Ar age (BOGARD *et al.*, 1993).

The parent body of howardites, eucrites, and diogenites (HED achondrites) experienced large scale melting and differentiation (MASON, 1962) in the earliest history of the solar system (PAPANASTASSIOU and WASSERBURG, 1969). The isotopic investigations of the HED achondrites point to prolonged cratering records on the HED parent body and suggest that it survived the cataclysm affecting the Moon ~3.8–4.0 Ga ago (BOGARD *et al.*, 1985, 1993; NYQUIST *et al.*, 1990). The youngest recorded impact melting occurred about 3.04 Ga ago (BOGARD *et al.*, 1985).

The thermal histories of monomict eucrites have been discussed in the context of their geological setting on the HED parent body (TAKEDA and GRAHAM, 1991). Because the pyroxenes in Y-792769 are individually homogenized, this breccia is a mixture of eucrites with a limited range of chemical compositions and cooling histories. The event which formed Y-792769 and Y-793164 also may have occurred after the pyroxenes in constituent fragments of monomict eucrites were homogenized in prior events. If the breccia formation age is older than the major impact cataclysm in the inner solar system, the metamorphic events accompanying formation of monomict eucrites may have occurred at times close to their crystallization ages of many eucrites.

To deduce the cratering history on the HED parent body, it is important that chronological information be obtained from several isotopic systems; thus ^{39}Ar-^{40}Ar, Rb-Sr and Sm-Nd isotopic studies of Y-792769 were undertaken in collaboration

with the mineralogic and petrographic investigations. Some of the results of our study of Y-792769 already have been published by BOGARD *et al.* (1993). This paper reports mineralogy and petrography of new polished thin sections (PTS) of Y-792769 and compares them to new data on Y-793164. Preliminary isotopic data for Y-793164 are given in this paper for comparison to those of Y-792769.

2. Samples and Methods

2.1. Samples

Polished thin sections (PTS) Y-793164,65–1 and ,63–1 were supplied by the National Institute of Polar Research (NIPR). PTS ,65–1 was made from a clast and is shown in Yanai and Kojima (1987; photo 292) and PTS ,63–1 represents a matrix

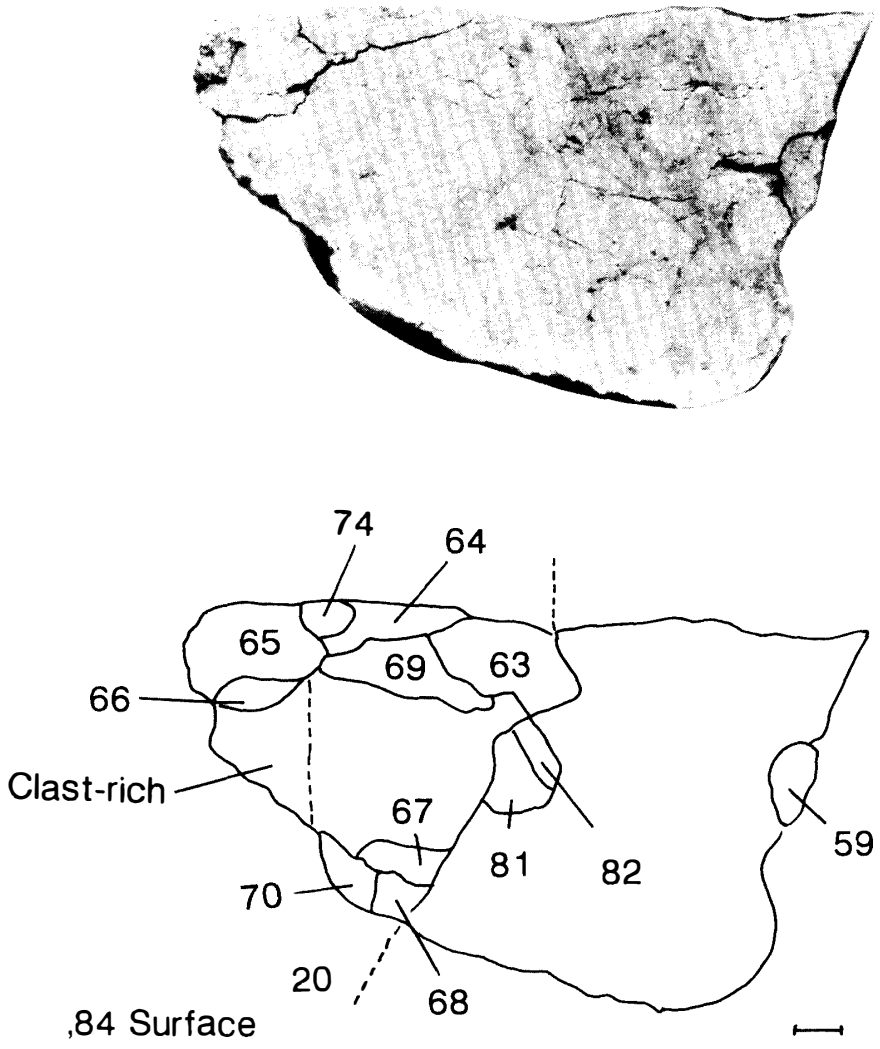

Fig. 1. Cut Surface of Y-792769,84 (top) with sample numbers indicated on the line drawing of the photograph (bottom). Chips ,68 and ,82 were studied by BOGARD et al. (1993) and chips ,59 and ,74 were used in this study. Chip ,82 is from the interior and ,68B1 is a part of a large lithic clast. The scale bar is 1 cm.

portion. Samples of Y792769 supplied by NIPR were taken from locations separated by several cm. Chips ,59 and ,74 were not far from the surface of the meteorite (Fig. 1). PTSs were prepared from these samples. Sub-samples for isotopic analysis also were prepared from these parent samples. Preparation of PTS and samples used for ^{39}Ar-^{40}Ar analyses and for Rb-Sr and Sm-Nd isotopic analyses are described in BOGARD *et al.* (1993). In the work reported in this paper, we studied PTSs Y-792769,74 and ,59 for mineralogical characterization, but data from PTSs ,62–2, 68 B1 and ,82 (interior chip) reported previously (BOGARD *et al.*, 1993) are also used for comparison.

The 0.450 g sample (Y-793164,70) used for isotopic analyses was composed of a uniformly dark gray matrix with a lighter colored clast adjacent to one surface. The clast was more friable than the matrix and clast material was separated from the matrix using a surgical knife. Visual inspection under a binocular microscope showed that little if any matrix was included with the clast material. This clast sample (Y-793164,70C) weighed 12.1 mg; a similarly sized sample was chosen at random from the matrix (Y-793164,70M; 13.1 mg). These samples were analyzed for Rb and Sr concentrations and Sr isotopic compositions. Some preliminary results of Sm and Nd analyses are utilized in this paper, but this work is incomplete and detailed results will be reported elsewhere.

2.2. *Mineralogical techniques*

Chemical compositions of minerals were determined by electron probe micro-analysis (EPMA) with the JEOL 733 Super Probe at the Ocean Research Institute of the University of Tokyo using the correction procedure based on the Bence-Albee method with the same parameters used by NAKAMURA and KUSHIRO (1970). The zoning profiles of pyroxenes were obtained by point analyses along a line at 10 μm intervals. The compositional variations of minerals in fine sintered matrices and in recrystallized areas were also obtained by this method. The chemical zoning of plagioclases were obtained by the same method but using a 5 μm interval. Chemical differences between individual mineral fragments were obtained by analyzing one to three points within fragments larger than about 100 μm in diameter.

2.3. *Rb-Sr procedures*

Isotopic studies of a small clast-rich chip of Y-793164 were performed at NASA/JSC. Standard methods of ion exchange chromatography were used to separate Rb and Sr for mass spectrometric analysis. The methods in recent use in the JSC laboratory were described by NYQUIST *et al.* (1990). Current Rb and Sr analytical blanks are ~15 pg Rb and ~55 pg Sr, and are negligible for the Y-793164 samples. The JSC/Finnigan-MAT 261 mass spectrometer was used for the Sr isotopic analyses and the JSC/NBS 6-inch mass spectrometer was used for the Rb analyses. Rb and Sr concentrations were determined by isotope dilution using a mixed ^{87}Rb-^{84}Sr spike. Twenty-one analyses of the NBS 987 isotopic standard yielded an average $^{87}Sr/^{86}Sr = 0.710251 \pm 22$ ($2\sigma_p$), in excellent agreement with earlier results measured in the JSC laboratory (NYQUIST *et al.*, 1990; BOGARD *et al.*,

1993).

3. Results

3.1. *Mineralogy of Y-793164*

The PTS Y-793164,65–1 is a part of a subophitic clast with a few lath-shaped

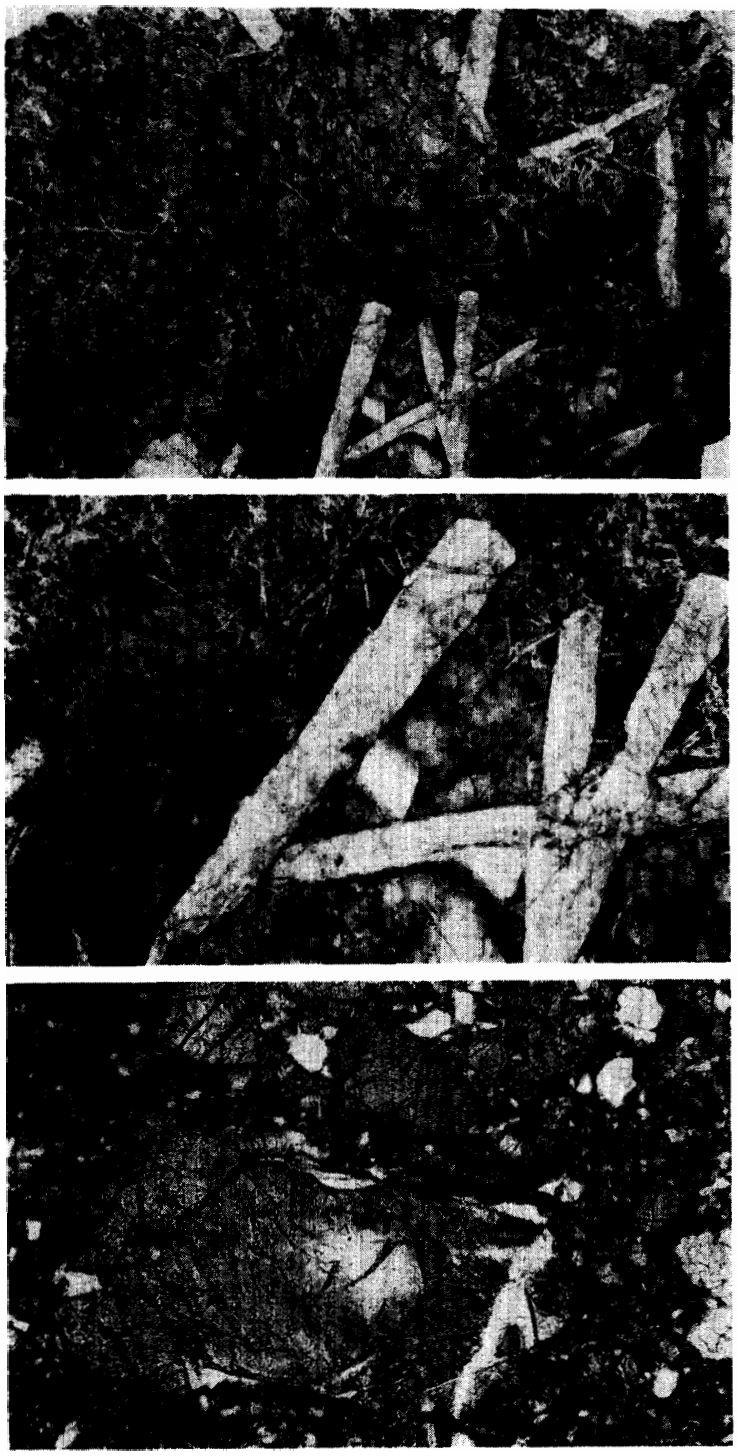

(a)

(b)

(c)

Fig. 2. Photomicrographs of Y-793164.

(a) Entire view of PTS Y-793164,65–1. Width is 3.3 mm.

(b) The largest lithic clast with acicular plagioclase in PTS ,65–1. Width is 1.3 mm.

(c) Lithic clast BS1 in PTS Y-793164,63–1. Width is 1.3 mm.

plagioclase crystals up to 1.1×0.34 mm in size. Pyroxene fills their interstices (Fig. 2a). About one half of the PTS preserves this texture (lithic clast BS1 in ,65–1). The most noteworthy textural feature of this clast is that large parts of the pyroxene contain aggregates of fine acicular plagioclase (Fig. 2b). The sizes of the acicular crystals range up to 0.15×0.05 mm in size and are far less than that of plagioclases

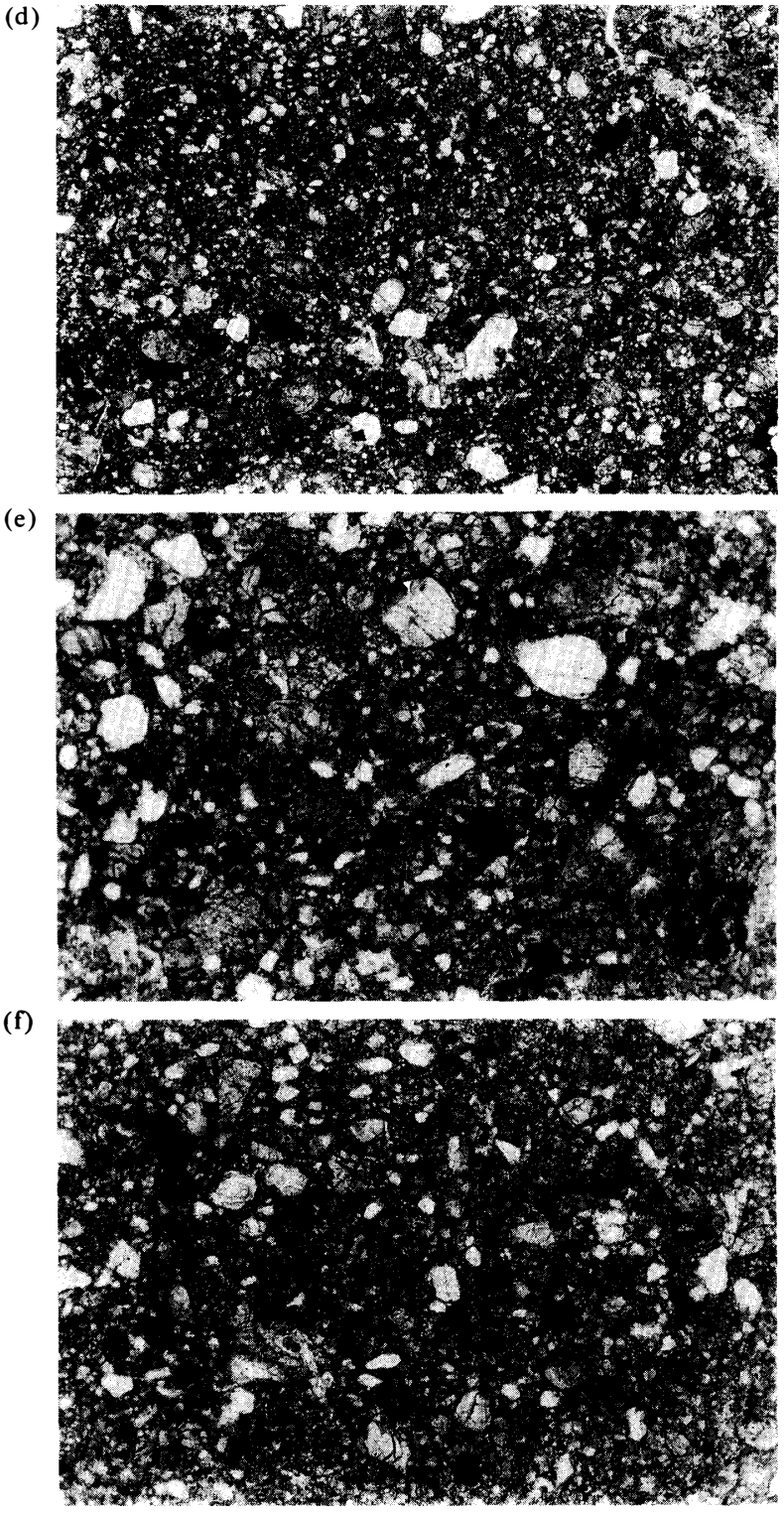

Fig. 2. Photomicrographs of Y-793164.
(d) Matrix-rich portion in PTS ,63–1 with few clasts. Width is 3.3 mm.
(e) Region rich in pyroxene fragments in PTS ,63–1. Width is 1.3 mm.
(f) Matrix with compact shock-sintered texture. Width is 1.3 mm.

in the original crystalline portion. This texture with acicular plagioclase is similar to that observed in a recrystallized portion of Juvinas (TAKEDA and YAMAGUCHI, 1991). Irregular aggregates of ilmenite 0.1 mm in diameter are present at the recrystallized mesostases.

PTS Y-793164,63–1 is quite different from ,65–1 and represents a matrix-rich

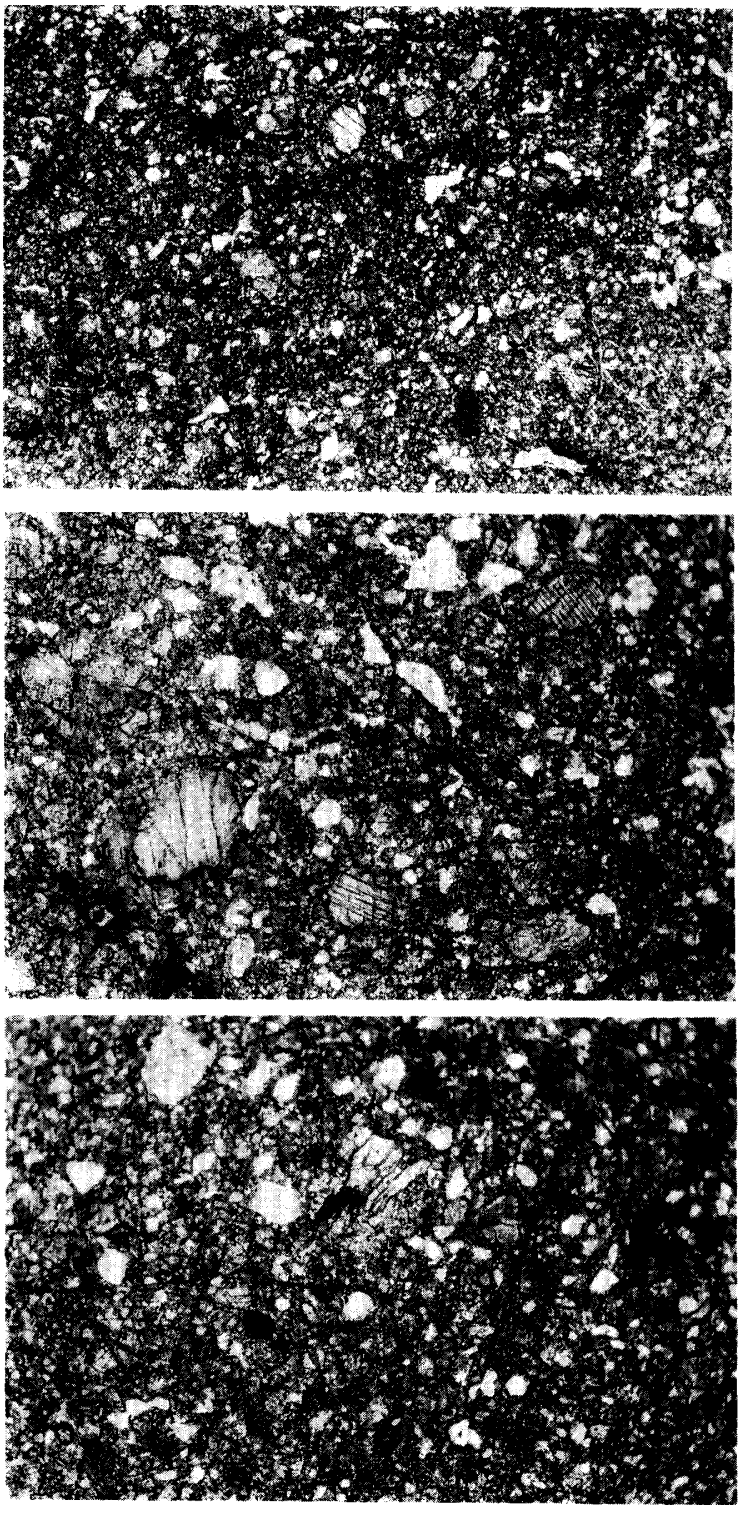

Fig. 3. Photomicrographs of Y-792769.

(a) A large view of Y-792769,74. Width is 3.3 mm.

(b) Pyroxene fragments in Y-792769,74A. Width is 1.3 mm.

(c) A matrix-rich portion of Y-792769,74. Width is 1.3 mm.

portion of this meteorite with a few lithic clast (Fig. 2c). Subrounded fragments of lithic and mineral clasts are set in a compact, dark yellowish brown matrix of very comminuted materials (Fig. 2d). The sizes of the fragments are finer than those in more typical polymict eucrites and the finest grains look like sintered glassy materials. The clast types include (a) a subophitic clast (BS1) as represented by PTS ,65–1, (b) a similar clast (BS1 in Fig. 2c) in PTS ,63–1, (c) a finer grained basaltic clast (BS3), (d) a pyroxene fragment (PF1) 0.72×0.42 mm in size with fine exsolution lamellae, and (e) a quickly cooled dark matrix-rich clast with acicular

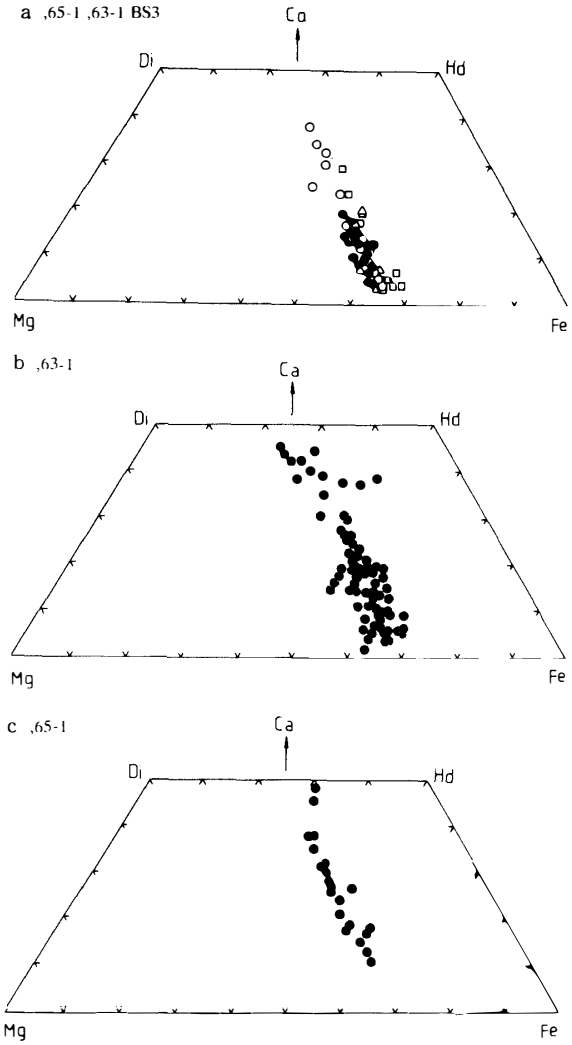

Fig. 4. Pyroxene quadrilaterals for Y-793164. (a) Open triangles, open and closed circles: different pyroxene crystals of a clast in ,65-1. Open squares: exsolution trends of pyroxene in basalt BS3 in ,63–1. (b) Closed circles: pyroxene fragments in matrix of Y-793164,63–1. (c) Closed circles: pyroxene matrix between acicular plagioclases in PTS ,65–1.

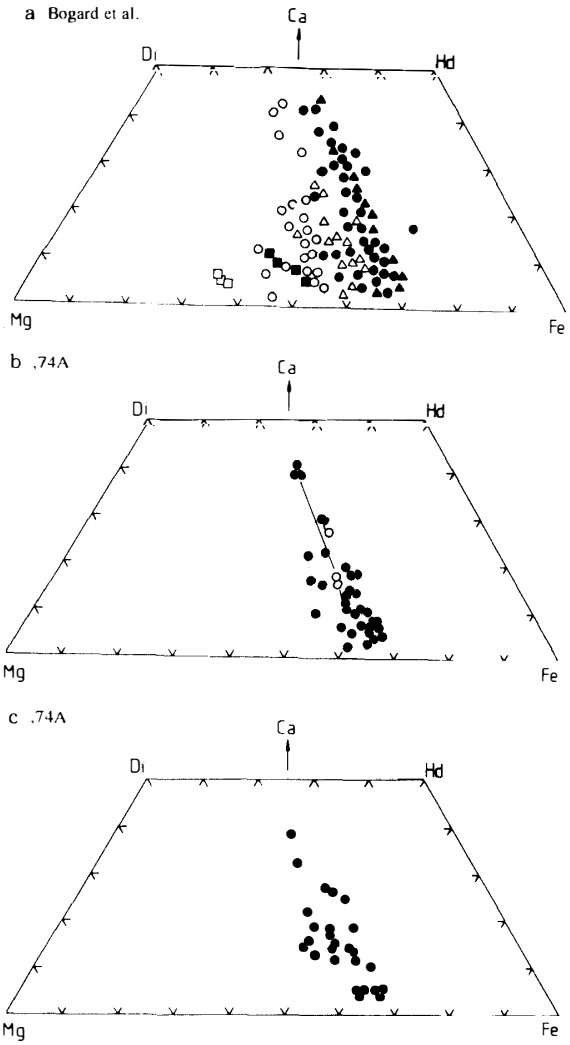

Fig. 5. Pyroxene quadrilaterals of Y-792769. (a) Y-792769,62–2 etc. include all pyroxene compositions given in diagrams of BOGARD et al. (1993), plus some additional analyses. Different symbols represent different clasts or pyroxene fragments. (b) Pyroxene fragments in matrix of Y-792769,74A. Open circles: bulk compositions of exsolved pyroxenes and the tie lines connect the lamella and host phases. (c) Compositions of fine matrix pyroxenes in Y-792769,74A.

Table 1a. Chemical compositions (wt%) of representative pyroxenes in Y-793164,65-1.

Clasts	BS1 Low-Ca (8)	BS1 High-Ca (49)	Rex1 matrix High-Ca (113)	Rex1 matrix Low-Ca (135)
SiO_2	47.1	49.8	50.0	47.5
TiO_2	0.33	0.22	0.42	0.77
Al_2O_3	0.96	0.89	0.81	0.40
FeO	34.0	19.8	22.1	33.9
MnO	1.03	0.57	0.74	1.05
MgO	10.5	9.60	9.17	9.40
CaO	3.62	17.9	16.4	5.00
Na_2O	0.02	0.03	0.04	—
K_2O	—	0.02	0.01	0.01
Cr_2O_3	1.45	0.14	0.26	1.78
V_2O_3	0.02	—	—	—
Total	99.07	99.03	99.98	99.77
Ca*	8.1	38.4	35.3	11.2
Mg	32.6	28.6	27.5	29.4
Fe	59.3	33.0	37.2	59.4

* Atomic %. BS1: clast

Clasts: BSI is clast name; Rexl matrix: Recrystallized portion in the matrix of clast BS1. Numbers in parentheses are analysis numbers of the Planetary Materials Database of University of Tokyo.

—: under detection limit.

Table 1b. Pyroxene compositions (wt%) of Y-793164,63-1.

Clasts	BS1 Core (1)	BS1 Rim (41)	BS3 Ca-poor (26)	BS3 Ca-rich (2)	Matrix Ca-poor (133)	Matrix Ca-rich (73)	Frag. PF1 Exsol. host (26)
SiO_2	49.3	48.0	48.0	48.3	49.0	47.9	48.5
TiO_2	0.14	0.19	0.21	0.38	0.24	0.82	0.16
Al_2O_3	1.51	0.60	0.23	0.51	0.76	1.25	0.48
FeO	32.2	35.7	37.5	25.7	37.1	22.7	37.0
MnO	1.03	1.21	1.27	0.81	1.12	0.66	1.14
MgO	12.41	10.15	9.36	8.78	9.92	8.59	9.83
CaO	2.64	2.16	2.03	13.06	1.35	14.91	1.77
Na_2O	0.02	0.01	—	0.06	0.04	0.05	0.02
K_2O	0.01	—	0.01	0.01	—	—	—
Cr_2O_3	0.60	1.18	0.60	0.79	0.28	3.48	0.26
V_2O_3	0.02	0.03	—	—	—	0.03	—
Total	99.84	99.20	99.21	98.31	99.84	100.35	99.22
Ca*	5.9	4.9	4.6	28.8	3.1	33.5	4.0
Mg	38.4	32.0	29.4	27.0	31.3	26.8	30.9
Fe	55.8	63.1	66.0	44.2	65.7	39.8	65.2

* Atomic %

Clasts: Clast names, matrix or fragment (Frag.).

Exsol. host: Host composition of exsolved pyroxene.

plagioclase crystals and dark devitrified impact melts. The matrix texture (Fig. 2f) is similar to that of Y-792769 (Fig. 3a, b, c) described below.

The pyroxene compositions of Y-793164 distribute on the more Fe-rich side of the pyroxene quadrilaterals (Fig. 4), than ordinary eucrites of type 4 to 5 (TAKEDA and GRAHAM, 1991), but show a range in *mg* numbers [$=(Mg\times100)/(Mg+Fe)$] $=30$ to 40, which is comparable to Y-792769 (Fig. 5). Some pyroxenes more Fe-rich than those in ordinary eucrites (MITTLEFEHLDT and LINDSTROM, 1993) are comparable to those in Lakangaon (MASON *et al.*, 1979). The pyroxene compositions of the clasts (*e.g.* ,63–1: BS3, ,65–1: BS1) show a homogenized trend with a small range in *mg* numbers (Fig. 4). The recrystallized portions with acicular plagioclase in ,65–1 show a more Ca-rich trend (Fig. 4c). The representative compositions of pyroxene are listed in Table 1.

The compositions of lath-shaped plagioclase crystals in PTS Y-793164,65–1 range from An_{80} to An_{90} (Fig. 6, Table 2), representing a crystallization trend from the original magma. The acicular crystals in PTS ,65–1 show a much wider range from An_{80} to An_{99}. The plagioclase compositions in clast BS3 in PTS ,63–1 have the same trend as in the lath-shaped crystals in PTS ,65–1. However, those of fragments in the matrix show a wider range from An_{90} to An_{70} (Fig. 6). Chemical compositions of other minerals are given in Table 3.

3.2. *Mineralogy of Y-792769*

PTSs of Y-792769 available for this study (,74 and ,59) consist mostly of

Table 2. Plagioclase compositions (wt%) of Y-793164,65-1 and ,63-1.

PTS	65–1	65–1	65–1	65–1	63–1	63–1
Clasts	BS1 Core (56)	BS1 Rim (33)	Acicular Ca-rich (105N)	Acicular Na-rich (97D)	BS1 Core (6)	BS3 Core (32)
SiO_2	47.8	46.6	47.6	46.9	49.8	49.2
TiO_2	0.01	0.08	0.01	0.01	0.03	0.09
Al_2O_3	33.5	32.8	33.5	33.7	31.6	31.1
FeO	0.20	0.80	0.29	0.28	0.46	0.63
MnO	—	0.04	—	—	—	0.01
MgO	0.01	0.24	0.01	0.01	0.06	0.02
CaO	17.15	17.51	17.40	17.22	16.32	16.29
Na_2O	2.08	1.26	1.41	1.80	1.43	1.47
K_2O	0.13	0.13	0.13	0.16	0.09	0.15
Cr_2O_3	—	0.06	—	—	—	—
Total	100.83	99.51	100.38	100.08	99.52	98.95
An*	81.4	87.8	86.6	83.3	85.9	85.2
Ab	17.8	11.5	12.7	15.7	13.6	13.9
Or	0.8	0.8	0.8	1.0	0.5	1.0

* Atomic %

Clasts: BS1 is a primary basalt portion and Acicular is an acicular one in PTS ,65–1.

—: under detection limit.

Table 3. Chemical compositions (wt%) of olivine, ilmenite and silica in Y-793164,63–1 and ,65–1.

PTS	63–1	65–1	63–1	65–1
Clasts	BS1	BS3	Frag.	Mesost.
Minerals	Olivine (31)	Ilmenite (1)	Ilmenite (108)	Silica (184)
SiO_2	31.6	0.02	0.02	95.5
TiO_2	—	53.0	52.9	0.04
Al_2O_3	0.06	0.04	0.10	0.27
FeO	58.6	45.6	44.5	1.59
MnO	1.38	0.86	0.80	0.04
MgO	7.33	0.28	0.52	0.52
CaO	0.07	0.07	0.07	0.81
Na_2O	0.01	0.01	0.02	—
K_2O	—	—	—	0.02
Cr_2O_3	0.03	0.03	0.01	—
Total	99.15	99.92	99.00	98.79
Fo*	18.2			
Fa	81.8			

* Atomic %
Clasts: Clast names, fragments (Frag.) or mesostasis (Mesost.).
—: under detection limit.

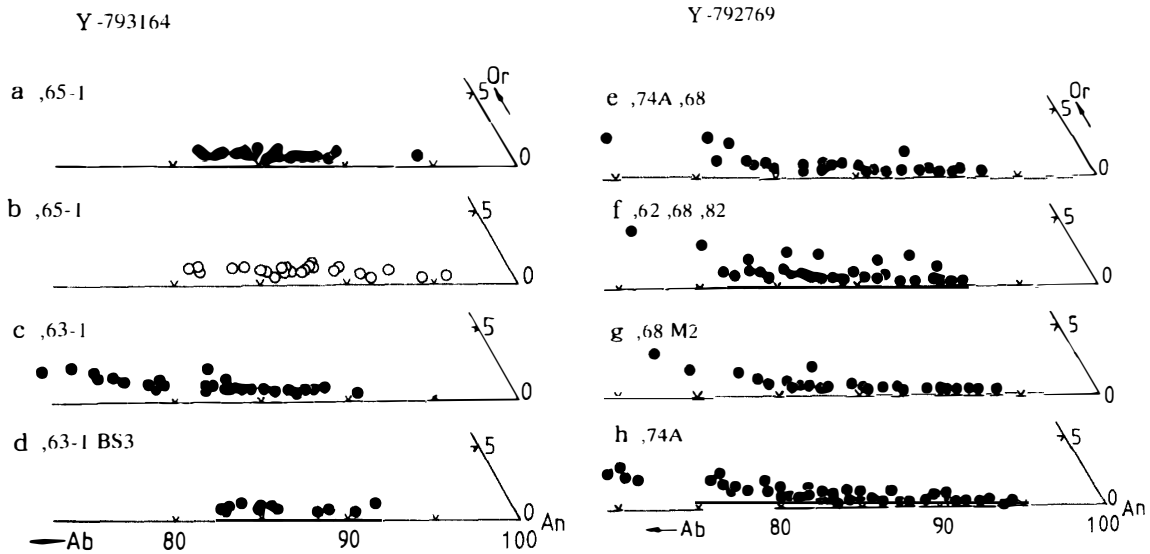

Fig. 6. Parts of the Or-Ab-An diagrams of plagioclases in fragments and clasts of Y-793164 (a to d) and Y-792769 (e to h). Numbers are An values. (a) Y-793164,65–1. Lath-shaped crystals in a crystalline clast. (b) Acicular plagioclases in Y-793164,65–1. (c) Plagioclase fragments in the matrix of Y-793164,63–1. (d) Clast BS3 in Y-793164,63–1. (e) Y-792769,74A and ,68. Representative plagioclases of fragments in the matrices and parts of the matrices. (f) Plagioclases in clasts in Y-792769,62, ,68 and ,82 by BOGARD *et al. (1993). (g) Plagioclase fragments in the matrices of Y-792769,68M2. (h) Plagioclase fragments in the matrices of Y-792769,74A.*

Table 4. Selected compositions (wt%) of Mg-rich pyroxene fragments in Y-792769,62–2.

PTS	62–2	62–2	62–2	62–2
Frag.	PF1	PF2	PF2	PF4
Remarks	Mg-rich (15)	Host (11)	Fe-rich (13)	Host (2)
SiO_2	52.2	49.1	47.2	50.5
TiO_2	0.15	0.20	0.80	0.50
Al_2O_3	1.04	0.92	0.77	0.55
FeO	20.7	30.5	31.6	30.4
MnO	0.72	1.06	1.02	0.96
MgO	21.2	11.77	11.39	15.13
CaO	3.18	4.93	5.14	1.78
Na_2O	0.05	0.02	0.02	0.01
Cr_2O_3	0.62	0.70	3.01	0.27
V_2O_3	—	—	0.02	—
Total	99.76	99.21	100.97	100.04
Ca*	6.5	10.9	11.2	3.8
Mg	60.4	36.3	34.7	45.3
Fe	33.1	52.8	54.1	50.9

* Atomic %
Frag.: Fragment names in BOGARD *et al.* (1993).
—: under detection limit.

Table 5a. Selected compositions (wt%) of pyroxene fragments in Y-792769,74A.

PTS	74A	74A	74A	74A	74A	74A
Frag.	PF1	EXP4	EXP4	EXP4	EXP6	EXP6
Remarks	Mg-rich (61)	Host (64)	Bulk (70)	Lamella (108)	Bulk (73)	Host (71)
SiO_2	49.3	49.2	49.3	48.4	49.3	50.0
TiO_2	0.39	0.32	0.62	0.71	0.53	0.52
Al_2O_3	1.27	0.75	0.82	2.01	0.99	1.21
FeO	26.8	32.4	29.6	18.24	25.5	24.2
MnO	0.69	0.87	0.78	0.47	0.75	0.66
MgO	11.8	10.94	10.33	9.00	9.35	9.22
CaO	7.57	4.80	7.07	18.40	12.13	13.29
Na_2O	0.04	0.03	0.03	0.07	0.01	0.04
K_2O	0.01	0.01	0.01	—	—	—
Cr_2O_3	1.17	0.16	0.47	1.51	0.55	0.46
V_2O_3	—	—	0.01	0.04	—	—
Total	99.05	99.46	99.05	98.88	99.14	99.63
Ca*	16.8	10.6	15.9	40.7	26.9	29.5
Mg	36.7	33.6	32.3	27.7	28.9	28.5
Fe	46.5	55.8	51.9	31.5	44.2	42.0

* Atomic %
Frag.: Fragment names; EXP: Exsolved pyroxene.
—: under detection limits.

fine-grained, compact matrix with a few subrounded lithic clasts and mineral fragments (Fig. 3a, b, c). The texture shown in Fig. 3c is identical to that of Y-793164,63–1 (Fig. 2f). The largest basaltic clast is less than 0.3 mm in diameter and has a subophitic texture of pigeonite and plagioclase. Other types of lithic clasts are present, but their abundances are lower than in common polymict eucrites. Fine veins of glassy materials run through parts of the matrix (Fig. 3c). Parts of the veins are sometimes thickened and tend to form small melt pockets. The importance of the presence of such glass veins was not emphasized in our previous paper (BOGARD *et al.*, 1993) with respect to the heat sources of the argon degassing. Some pyroxenes show exsolution (Fig. 3b) and the homogenized Mg/Fe distribution trends of ordinary eucrites, but the *mg* numbers often differ slightly from one clast to the other.

The matrix (*e.g.*, PTS Y-792769,74 and ,59) shows dark, yellowish fine-grained sintered textures lacking very fine fragments (Fig. 3c). Small, subrounded fragments of pyroxene and plagioclase are occasionally scattered in the matrices (Fig. 3b), but the size distribution (<0.1 mm in diameter) is different from that of less sorted mineral fragments in normal polymict eucrites, (<0.01 to 3 mm), such as Y-75011 (DELANEY *et al.*, 1984). The fine-grained, sintered material gives the matrix a dark glassy appearance.

Table 5b. Representative pyroxene compositions (wt%) in clasts and matrices of Y-792769 ,62–2 ,82A, and ,72A.

PTS	62–2	62–2	62–2	82A	82A	62–2	72A
Clasts	SB1	SB1	GB2	BS8	BS8	Matrix	Matrix
Remarks	Host	Lamella	Host	Host	Lamella	High-Ca	Low-Ca
	(10)	(7)	(67)	(3)	(4)	(103)	(254)
SiO_2	48.6	47.9	48.3	47.1	49.8	49.8	49.6
TiO_2	0.07	0.61	0.38	0.26	0.03	0.53	0.29
Al_2O_3	0.14	0.75	0.57	0.48	0.91	1.23	0.45
FeO	37.0	27.1	32.9	34.6	16.40	17.81	35.2
MnO	1.11	0.86	1.12	1.19	0.55	0.50	1.15
MgO	9.22	7.92	10.89	11.19	9.92	9.47	11.30
CaO	2.27	12.49	4.47	1.22	19.81	19.07	2.15
Na_2O	—	0.04	0.01	0.02	0.05	0.03	—
K_2O	0.01	—	—	—	0.09	0.01	—
Cr_2O_3	0.21	1.56	1.29	0.30	—	0.56	0.06
V_2O_3	—	—	—	—	0.40	0.02	—
Total	98.69	99.28	99.96	96.35	98.17	99.03	99.97
Ca*	5.2	28.0	9.9	2.8	42.7	41.3	4.7
Mg	29.2	24.7	33.4	35.6	29.7	28.5	34.7
Fe	65.7	47.4	56.7	61.6	27.6	30.1	60.6

* Atomic %
Clasts: Clast names used in BOGARD *et al.* (1993) and Matrices.
Remarks: Host and Lamella are for exsolved pyroxenes.
—: under detection limits.

Table 6a. Representative plagioclase compositions (wt%) of lithic clasts in Y-792769,62–2 and ,82A.

PTS	62–2	62–2	62–2	82A	82A
Clasts	SB1 Ca-rich (40)	GB2 Ca-rich (71)	GB2 Na-rich (72)	B1 Ca-rich (15)	B1 Na-rich (22)
SiO_2	44.9	47.9	49.4	47.8	48.8
TiO_2	—	—	—	—	0.02
Al_2O_3	34.6	30.6	31.4	32.5	31.4
FeO	0.05	0.44	0.23	0.12	0.38
MnO	—	0.01	—	0.03	0.02
MgO	0.02	0.18	0.03	0.04	0.02
CaO	18.20	16.79	15.55	16.84	15.96
Na_2O	1.14	2.08	2.62	1.99	2.26
K_2O	0.07	0.17	0.26	0.17	0.17
Cr_2O_3	0.05	0.02	0.05	—	—
Total	99.05	98.18	99.58	99.47	99.12
An*	89.4	80.9	75.5	81.6	78.8
Ab	10.1	18.1	23.0	17.4	20.2
Or	0.4	1.0	1.5	1.0	1.0

* Atomic %
Clasts: SB1, GB2, and B1 are clast names used in BOGARD *et al.* (1993) and fragments (Frag.).
—: under detection limits.

Table 6b. Representative plagioclase compositions (wt%) of fragments in Y-792769,82A and ,74A.

PTS	82A	82A	74A	74A	74A	74A	74A
	Frag. Ca-rich (103)	Frag. Na-rich (94)	Frag. Ca-rich (44)	Frag. Interm. (43)	Frag. (bulk) Na-rich (34, 35)	Frag. Na-rich (41)	Glass (10–26)
SiO_2	43.6	51.8	45.2	47.3	51.6	51.6	49.9
TiO_2	—	0.03	0.00	0.01	0.02	0.00	0.84
Al_2O_3	35.2	30.1	35.3	33.2	30.2	30.7	12.30
FeO	0.21	0.34	0.28	0.35	0.32	0.29	18.65
MnO	—	0.02	0.00	0.00	0.00	0.00	0.55
MgO	0.05	0.03	0.02	0.04	0.06	0.02	5.53
CaO	19.22	13.82	19.05	16.87	13.92	14.32	10.70
Na_2O	0.66	3.46	0.78	1.89	3.27	3.24	0.65
K_2O	0.05	0.38	0.06	0.12	0.40	0.42	0.05
Cr_2O_3	—	—	0.00	0.04	0.02	0.02	0.25
Total	99.00	100.05	100.71	99.93	99.90	100.62	99.38
An*	93.9	67.3	92.8	82.6	67.9	69.3	—
Ab	5.9	30.5	6.9	16.7	28.9	28.3	—
Or	0.3	2.2	0.3	0.7	2.3	2.4	—

* Atomic %
Frag.: Fragments.
—: under detection limits.

The chemical compositions of pyroxene fragments (Fig. 4b) differ from those of previous studies (BOGARD *et al.*, 1993; TAKEDA, 1991) in that the Mg-rich components (Table 4) are missing. Some pyroxenes have compositional trends similar to the trend for the Lakangaon eucrite (MASON *et al.*, 1979), one of the most Fe-rich trends found for eucrites. Compositions of pyroxene in the matrix distribute in the same manner as those from the lithic clast (Fig. 5). Representative pyroxene compositions in Y-792769 are given in Table 5 and are compared with those studied previously (BOGARD *et al.*, 1993). The plagioclase compositions (Table 6) distribute in the range reported previously (BOGARD *et al.*, 1993). The Fe-rich olivine veins similar to that found in Y-793164 have not been found in Y-792769, but a very small grain of Fe-rich olivine has been detected in the matrix of Y-792769,74A by the SEM technique.

3.3. Rb-Sr analytical results

The analytical results of the Rb and Sr analyses of the Y-793164,70 matrix and clast samples are given in Table 7 where they are compared to analyses of two different matrix samples of Y-792769, from subsamples ,68 and ,82 (Fig. 1). The Y-792769 subsamples were taken from locations separated from one another by ~4.5 cm. The Rb and Sr concentrations in the Y-793164 clast and matrix samples are very similar to one another. The Sr concentrations in these samples are also similar to those in the Y-792769 subsamples, but the Rb concentrations are ~17–37% higher than in the Y-792769 samples. The comparatively high Rb concentrations of both sets of samples are consistent with the observation of WOODEN *et al.* (1983) that Antarctic polymict eucrites have generally higher Rb contents than non-Antarctic ordinary eucrites. WOODEN *et al.* (1983) also observed that the consistently high Sr, Sm, and Nd concentrations of the Yamato eucrites identify them as a closely related group distinct from most other eucrites. The Sr concentrations of both Y-792769 and Y-793164 lie within the range of values reported by WOODEN *et al.* (1983) for a larger suite of Yamato eucrites. The ten samples for which WOODEN *et al.* (1983)

Table 7. Comparison of Rb-Sr analytical data for Y-793164 and Y-792769.

Sample	Wt. (mg)	Rb (ppm)	Sr (ppm)	$^{87}Rb/^{86}Sr$[a]	$^{87}Sr/^{86}Sr$[b]	T_{BABI}[c] (Ga)
Y793164,70M[e]	13.05	0.4071	77.75	0.01517±7	0.699944±14	4.39±0.08
Y793164,70C[f]	12.10	0.4123	76.14	0.01566±7	0.699997±23	4.49±0.11
Y792769,68[g]	19.7	0.3031	79.06	0.01109±6	0.699780±12	4.97±0.10
Y792769,82[g]	26.11	0.3492	83.56	0.01209±6	0.699814±16	4.76±0.11
NBS 987 (N=21)					0.710251±22[d]	

[a] Error limits apply to the last digits and include a minimum uncertainty of 0.5% plus 50% of the blank correction for Rb and Sr, added quadratically.

[b] Normalized to $^{88}Sr/^{86}Sr=8.37521$. Uncertainties refer to last digits and are $2\sigma_m$ where $\sigma_m=[\sum(m_i-\mu)^2/N(N-1))]^{1/2}$ for N measurements m_i with mean μ.

[c] Model ages relative to BABI=0.69898. $\lambda(^{87}Rb)=1.402\,Ga^{-1}$.

[d] Error limits are $2\sigma_p$ where $\sigma_p=[(m_i-\mu)^2/(N-1)]^{1/2}$ for N measurements m_i with mean value μ.

[e] Matrix. [f] Clast. [g] BOGARD *et al.* (1993).

report whole rock analyses have average Rb and Sr contents of 0.355 ± 0.16 ppm ($2\sigma_p$) and 81.1 ± 6.3 ppm ($2\sigma_p$), respectively, illustrating the extraordinarily tight grouping of Sr concentrations in these samples. Inspection of Table 7 shows that the Y-792769 matrix samples have Rb and Sr concentrations which are very near the Yamato group averages. However, the Y-793164 samples deviate from the group average by $\sim 1\sigma_p$ towards both higher Rb concentrations and lower Sr concentrations.

The argon data given by BOGARD *et al.* (1993) indicate that clast Y-792769,68 was almost completely degassed of its radiogenic ^{40}Ar at 3.99 ± 0.04 Ga ago and has not been substantially heated since that time. This dated event has been interpreted as being the same one which caused the sintered texture observed in the matrix and inferred to be the result of shock compaction during formation of the breccia (BOGARD *et al.*, 1993). The new PTS ,74 shows more numerous glassy veins, the presence of which should have significantly contributed to argon degassing.

4. Discussion

4.1. Pairing of Y-792769 and Y-793164

The shock-sintered texture of matrices of these two meteorites (*i.e.* PTS Y-792769,82A,M2, ,74A and Y-793164,63–1) is a very characteristic feature not present in other polymict eucrites. Comparisons of the mineralogic compositions obtained for Y-792769 and Y-793164 indicate that these two eucrites are distinct from members of other groups recovered from Antarctica (TAKEDA, 1991) and support the proposed pairing by MIURA *et al.* (1993). Differences between Y-792769,82A,M2, ,74A (Fig. 5c) and Y-793164,63–1 (Fig. 2f) are consistent with the small variations in textures and compositions of matrices within a single large brecciated meteorite. The monomict nature of Y-793164 reported by MITTLEFEHLDT and LINDSTROM (1993) for their sample may be interpreted as due to such variations.

The textural variations of the clasts suggest that the breccias are polymict, but the compositional variations of their pyroxenes are smaller than for other polymict eucrites (TAKEDA, 1991). However, the textures and compositions of large lithic clasts and pyroxene fragments in Y-792769,62–2 and Y-793164,65–1 are different from small fragments in the matrices of these meteorites. For example, Mg-rich pyroxenes in Y-792769,62–2 (Table 4) and pyroxenes with acicular plagioclase crystals in basaltic clast BS1 of Y-793164,65–1 (Table 1) are not present in the matrices. The compositional ranges are smaller for Y-793164,63–1 than for Y-792769,62–2. Although the Rb-Sr isotopic data (given below) do not strongly support pairing of these two meteorites to the exclusion of other Yamato eucrites, the observed isotopic differences also may be due to local heterogeneities.

Apart from the textural and compositional heterogeneity described above, major parts of these eucrites, *i.e.*, the compact sintered fine-grained matrix and small lithic clasts and subrounded mineral fragments, show only small ranges in mineral compositions. It appears that these breccias contain monomict eucritic materials

with small pyroxene compositional ranges which were homogenized prior to incorporation into the breccias. The sample of Y-793164 studied by MITTLEFEHLDT and LINDSTROM (1993) may have been either homogeneous matrix or a brecciated monomict clast. Further geochemical studies are required to evaluate these alternatives.

4.2. Isotopic consideration

Figure 7 summarizes Rb and Sr concentrations for a larger set of Antarctic polymict eucrites, including data from the JSC laboratory for eucrites from Allan Hills and Elephant Moraine as well as the data of WOODEN *et al.* (1983) for the Yamato eucrites. This figure reinforces the earlier conclusions of WOODEN *et al.* (1983) that Yamato eucrites are closely grouped in Rb and Sr concentration and that the concentrations of these elements tend to be higher in the Yamato eucrites than in other eucrite groupes. The Y-792769 data show that this meteorite is clearly typical of Yamato eucrites, whereas the Y-793164 data lie at the edge of the field defined by the Yamato group.

The Rb-Sr isotopic data of Y-793164 and Y-792769 are shown in an isochron diagram in Fig. 8 in comparison to data for other Antarctic polymict eucrites. Although data for both samples plot approximately along a 4.56 Ga reference isochron through initial $^{87}Sr/^{86}Sr$ for angrites as measured in the JSC laboratory (NYQUIST *et al.*, 1994), the distance between the two pairs of samples measured along the isochron is considerably greater than the distance between the members of either pair. We thus conclude that the probability that the bulk Rb-Sr systematics of the two meteorites differ exceeds the probability that they are the same. These observations do not support the suggestion that the two meteorites represent a

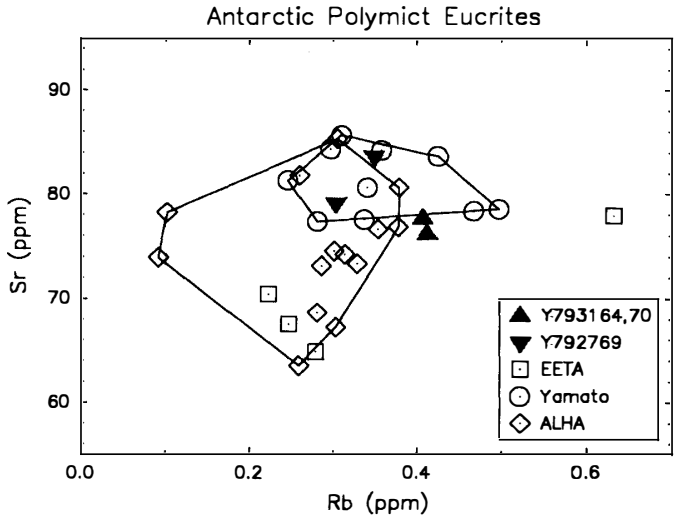

Fig. 7. Rb and Sr abundances in Antarctic polymict eucrites. All data are from the JSC laboratory. The data for the Yamato eucrites tend to higher Rb and Sr abundances than data for other Antarctic and non-Antarctic meteorites, as first noted by WOODEN et al. (1983). Data for Y-792769 are completely typical of the Yamato group, whereas data for Y-793164 lie near the present boundary of the group.

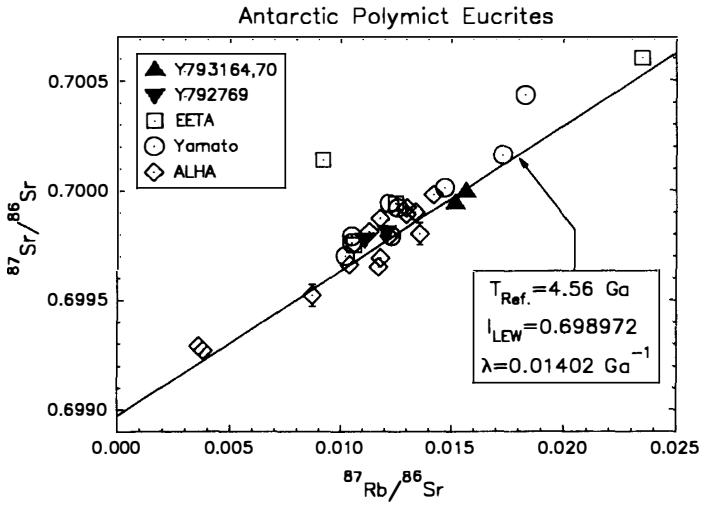

Fig. 8. Rb-Sr isotopic systematics of Antarctic polymict eucrites summarized in an isochron plot. All data are from the JSC laboratory. The Rb-Sr isotopic systematics of Y-792769 plot near the center of the Yamato group. The Y-793164 data plot at slightly higher $^{87}Rb/^{86}Sr$ and $^{87}Sr/^{86}Sr$ values and appear to be resolved from those of Y-792769 (see text).

paired fall. If, indeed, the latter is the case, then the compositional differences between the locations of the sample pairs in the parent (pre-atmospheric) meteoroid exceeds that observed over intervals of a few cm within each member of the pair. This appears to be true even though maximum diversity within a given specimen was sought by taking matrix samples separated by comparatively large distances in Y-792769, and by sampling both clast and matrix in Y-793164.

The Rb-Sr isotopic data also provide a hint that Y-792769 and Y-793164 experienced different thermal environments. This conclusion should be regarded as tentative until Ar-Ar age dating can be completed. However, the Rb-Sr model ages for the two meteorites differ in excess of the estimated analytical errors (By convention, Table 7 lists model ages relative to BABI=0.69898 (PAPANASTASSIOU and WASSERBURG, 1969), whereas the reference isochron in Fig. 8 is shown relative to the initial $^{87}Sr/^{86}Sr$ measured in the JSC laboratory for the LEW86010 angrite, 0.698972±8 (NYQUISTt *et al.*, 1994), and is thus directly applicable to the JSC data). The high model age of Y-792769 (Table 7), or, equivalently, its displacement above the reference isochron in Fig. 8, is suggestive of Rb loss via volatilization early in the meteorite's history. This does not appear to have occurred for Y-793164. Thus, in spite of the general compositional and isotopic similarity between Y-792769 and Y-793164, the Rb-Sr data suggests that they are not composed of identical material and did not have identical histories. This, of course, does not rule out the possibility that they were ejected from the parent body in the same event, as suggested by the similar exposure ages of the two meteorites. It is likely that the small differences in the Rb-Sr isotopic characteristics of the two meteorites is due to small-scale textural and compositional heterogeneities as discussed above.

4.3. *Cratering history of the HED parent body*

The last thermal event, which produced the sintered texture and formed the Y-792769 breccia, is determined by a well-defined ^{39}Ar-^{40}Ar age of 3.99±0.04 Ga (BOGARD *et al.*, 1993). The complete resetting of the ^{39}Ar-^{40}Ar age is consistent with the presence of the glassy veins and textures viewed in the transmission electron microscope (TEM) which suggest that shock compaction converted part of the matrix plagioclase to maskelynite (BOGARD *et al.*, 1993). Sm-Nd data for Y-792769 define an apparent isochron corresponding to an age of 4.23±0.12 Ga, which probably reflects partial resetting of the Sm-Nd system during breccia formation (BOGARD *et al.*, 1993). New data for the Sm and Nd concentrations of a bulk sample of Y-793164 matrix are 1.92 and 5.64 ppm, respectively, and are very similar to Sm and Nd concentrations in a bulk sample of Y-792769,68 (BOGARD *et al.*, 1993). The Nd-isotopic compositions of these two samples are also very similar. Both observations are consistent with pairing of the two meteorites, but do not provide independent information about the thermal history of the samples.

Shock-induced brecciation and sintering of Y-792769 and Y-793164 presumably resulted from impact of a large meteoroid on the HED parent body. The nearly homogeneous distribution of the matrix within the entire meteorite and the presence of the TEM-scale exsolution in the matrix pyroxenes and of maskelynitized plagioclases in the matrix suggest that the breccia was produced in a single cratering event. The nearly uniform compositions of the matrix pyroxenes also indicate some degree of subsolidus annealing, which may have occurred at the same time the Ar-Ar age was reset. Alternatively, the pyroxenes in the original lithologies already may have had only limited compositional ranges before the breccia was lithified.

According to the geological setting suggested for the HED parent body (NYQUIST *et al.*, 1986; TAKEDA and GRAHAM, 1991), the original components of Y-792769 may have been derived from previously homogenized eucritic lithologies, where the original monomict eucrites parental to some clasts were thermally metamorphosed. Then, components with different pyroxene chemistries were mixed by the major impact event, which reset the ^{39}Ar-^{40}Ar age. This interpretation implies that metamorphic events homogenized the precursor monomict eucrites prior to the major cratering event of 3.99 Ga. An alternative scenario that could partly explain the petrologic data would be homogenization of a polymict breccia before the last shock event. However, Mg-rich pyroxene fragments in the Fe-rich matrix do not show evidence of Fe migration by diffusion at the rims as might be expected for *in situ* pyroxene homogenization.

The ^{39}Ar-^{40}Ar ages of the impact events in which Y-792769 and monomict eucrites such as Millbillillie (YAMAGUCHI *et al.*, 1993) and Y-75011 (BOGARD, personal communication) were formed are similar to the ^{39}Ar-^{40}Ar ages of many lunar highland rocks which had their isotopic systematics reset by large cratering events early in lunar history (BOGARD and GARRISON, 1993). The ^{39}Ar-^{40}Ar ages determined for Y-792769 and Y-75011 (4.0 Ga), however, are slightly older than the usually accepted times of formation of the large Imbrium and Serenitatis basins on the moon, but the age of Millbillillie (3.55 Ga) is younger than the last known time

of lunar basin formation. Thus impact cratering on the HED parent body was both intense and of long duration.

In summary, (1) mineralogy and petrology of Y-792769 and Y-793164 indicate that these eucrites show generally similar shock-sintered textures and mineralogical compositions and support their proposed pairing, except for the apparently greater abundance of Mg-rich materials in Y-792769; (2) a few types of lithic clasts represent equilibrated eucrites with slightly different pyroxene *mg* numbers; (3) a lithic clast with pyroxenes including acicular plagioclase has been observed and is similar to one found in Juvinas; (4) the presence of glassy veins in the matrices of Y-792769 is additional evidence of a heat source for degassing Ar; (5) events which homogenized pyroxenes in different lithologies may have taken place before the impact event 3.99 Ga ago recorded in Y-792769; and (6) Rb-Sr data of Y-793164 and Y-792769 neither support nor reject the proposed pairing of these meteorites. Preliminary Sm-Nd data weakly support their pairing.

Acknowledgments

We thank NIPR for the meteorite samples and Drs. H. KOJIMA and K. YANAI for the allocation diagram of a large cut surface. A part of this paper was written while one of the authors (H.T.) was a visiting scientist at the Lunar and Planetary Institute, Houston, U.S.A. and the support of that institute is gratefully acknowledged. This work also was supported in part by a Grant-in-Aid for Scientific Research from the Ministry of Education, Science and Culture of Japan and in part by funds from the Cooperative Program (No. 33) provided by Ocean Research Institute, University of Tokyo. We are indebted to Dr. D. W. MITTLEFEHLDT and Prof. Y. IKEDA for critical reading of the manuscript, Dr. T. ISHII of Ocean Research Institute, University of Tokyo and Mr. H. YOSHIDA of the Geological Institute, University of Tokyo for their help in microanalysis, Dr. H. MORI for fruitful discussion, and Drs. B. M. BANSAL and C.-Y. SHIH, Mr. H. WIESMANN, D. H. GARRISON, O. TACHIKAWA, and Mrs. M. OTSUKI and K. HASHIMOTO for their technical assistance.

References

BOGARD, D. D. and GARRISON, D. H. (1993): ^{39}Ar-^{40}Ar of eucrites and howardites and the early bombardment of the HED parent body. Meteoritics, **28**, 325–326.

BOGARD, D. D., TAYLOR, G. J., KEIL, K., SMITH, M. R. and SCHMITT, R. A. (1985): Impact melting of the Cachari eucrite 3.0 Gy ago. Geochim. Cosmochim. Acta, **49**, 941–946.

BOGARD, D. D., NYQUIST, L. E., TAKEDA, H., MORI, H., AOYAMA, T., BANSAL, B., WIESMANN, H. and SHIH, C.-Y. (1993): Antarctic polymict eucrites Yamato 792769 and cratering record on the HED parent body. Geochim. Cosmochim. Acta, **57**, 2111–2121.

DELANEY, J. S., PRINZ, M. and TAKEDA, H. (1984): The polymict eucrites. Proc. Lunar Planet. Sci. Conf. 15th, C251–C288 (J. Geophys. Res., **89**, Suppl.).

MASON, B. (1962): Meteorites. New York, Wiley 274 p.

MASON, B., JAROSEWICH, E. and NELEN, J. A. (1979): The pyroxene-plagioclase achondrites. Smithson. Contrib. Earth Sci., **22**, 27–45.

MITTLEFEHLDT, D. W. and LINDSTROM, M. M. (1993): Geochemistry and petrology of a suite of ten Yamato HED meteorites. Proc. NIPR Symp. Antarct. Meteorites, **6**, 268–292.

MIURA, Y., NAGAO, K. and FUJITANI, T. (1993): ^{81}Kr terrestrial ages and grouping of Yamato eucrites based on noble gas and chemical compositions. Geochim. Cosmochim. Acta, **57**, 1857–1866.

NAKAMURA, Y. and KUSHIRO, I. (1970): Compositional relations of coexisting orthopyroxene, pigeonite and augite in a tholeiitic andesite from Hakone volcano. Contrib. Mineral. Petrol., **26**, 265–275.

NYQUIST, L. E., TAKEDA, H., BANSAL, B. M., SHIH, C.-Y, WIESMANN, H. and WOODEN, J. L. (1986): Rb-Sr and Sm-Nd internal isochron ages of a subophitic basalt clast and a matrix sample from the Y75011 eucrite. J. Geophys. Res., **91**, 8137–8150.

NYQUIST, L. E., BOGARD, D. D., WIESMANN, H., BANSAL, B. M., SHIH, C.-Y. and MORRIS, R. M. (1990): Age of a eucrite clast from the Bholghati howardite. Geochim. Cosmochim. Acta, **54**, 2195–2206.

NYQUIST, L. E., BANSAL, B. M., WIESMANN, H. and SHIH, C.-Y. (1994): Nd, Sr, and Cr isotopic studies of the LEW86010 and Angra dos Reis meteorites and the chronology of the angrite parent body. submitted to Meteoritics.

PAPANASTASSIOU, D. A. and WASSERBURG, G. J. (1969): Initial strontium isotopic abundances and the resolution of small time differences in the formation of planetary objects. Earth Planet. Sci. Lett., **5**, 361–376.

TAKEDA, H. (1991): Comparisons of Antarctic and non-Antarctic achondrites and possible origin of the differences. Geochim. Cosmochim. Acta, **55**, 35–47.

TAKEDA, H. and GRAHAM, A. L. (1991): Degree of equilibration of eucritic pyroxenes and thermal metamorphism of the earliest planetary crust. Meteoritics, **26**, 129–134.

TAKEDA, H. and YAMAGUCHI, A. (1991): Recrystallization and shock textures of old and new samples of Juvinas in relation to its thermal history. Meteoritics, **26**, 400–401.

WOODEN, J. L., TAKEDA, H., NYQUIST, L. E., WIESMANN, H. and BANSAL, B. (1983): A Sr and Nd isotopic study of five Yamato polymict eucrites and a comparison to other Antarctic and ordinary eucrites. Mem. Natl Inst. Polar Res., Spec. Issue, **30**, 315–322.

YAMAGUCHI, A., TAKEDA, H., BOGARD, D. and GARRISON, D. (1993): Textural variations and impact history of the Millbillillie eucrite. Meteoritics, **29**, 16–24.

YANAI, K. and KOJIMA, H. (1987): Photographic Catalog of Antarctic Meteorites. Tokyo, Natl Inst. Polar Res., 298 p.

(Received August 18, 1993; Revised manuscript received January 31, 1994)